THE EDDY CURRENT LOSSES OF HIGH-SPEED SOLID ROTOR INDUCTION MACHINE AS FUNCTION OF THE RADIAL AIR-GAP LENGHT

Jan Bárta

Doctoral Degree Programme (2), FEEC BUT

E-mail: jan.barta@phd.feec.vutbr.cz

Supervised by: Čestmír Ondrůšek

E-mail: ondrusek@feec.vutbr.cz

Abstract: This paper introduces that the appropriately selected air-gap width have major impact in terms of efficiency for high-speed induction machines. Machine of interest is high-speed solid rotor cage induction machine intended for helium turbo-circulator. Proposed study is done from electromagnetic and thermal point of view. Presented results can be used as a guideline for air-gap length selection for others high-speed solid rotor induction machines.

Keywords: AC machine; High-speed drive; Induction motors; Finite element analysis

1. INTRODUCTION

Rapid grow can be noticed in development, research and applications of high-speed electrical machines in recent years. High efficiency level of new high-speed motors has to be reached to minimize their energy losses.

Electrical machine under investigation is shown in Fig. 1. This machine is three-phase, 2 poles high-speed solid rotor cage induction machine (HSSRCIM). Short-pitched double-layer winding for suppressing 5th and 7th air-gap flux density harmonics is distributed within 12 stator slots. Solid rotor structure instead of laminated one is used due to high centrifugal forces. To achieve necessary centrifugal force resistance the containment sleeve is fitted over the short-circuit rings. Parameters of the machine under investigation are listed in table I.

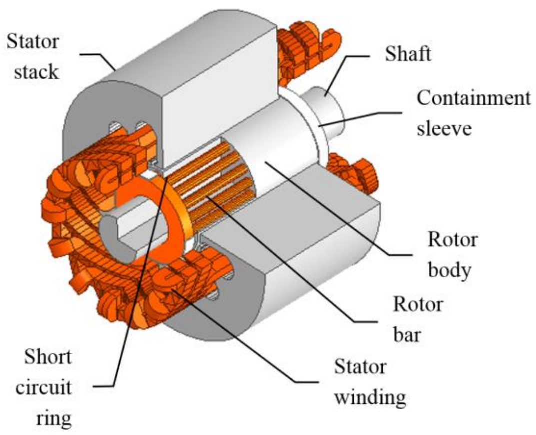

Figure 1: Solid rotor cage induction machine 6 kW, 120 000 rpm

Specification	Unit	Rating values
Number of pole pairs		1
Number of phases		3
Number of stator slots		12
Number of rotor slots		18
Stator external diameter	mm	90
Stator inner diameter	mm	32.5
Active length	mm	50
Rotor diameter	mm	30.7
Rated line-to-line voltage	V	350
Stator winding connection		Wye
Stator stack material		M250-35A
Rotor stack material		41CrMo4
Squirrel cage material		Glidcop – Al 15

Table 1: Main parameters of machine under investigation

2. THEORETICAL BACKGROUND

High-speed electrical machines are powered from high-frequency power sources. If we considered constant magnetic flux in the air-gap, then we can write following equation

$$P_{loss} = P_{fund} + P_{hyst} + P_{eddy} + P_{fric} \approx k_{fund} + k_{hyst}\omega + k_{eddy}\omega^2 + k_{fric}\omega^3 \quad (1)$$

where P_{loss} are electrical machine total losses, P_{fund} are losses nondependent on frequency (e.g. additional losses), P_{hyst} are losses dependent on frequency (e.g. hysteresis losses), P_{eddy} are losses dependent on square of frequency (e.g. eddy current losses) and P_{fric} are losses dependent on cube of frequency (e.g. friction losses). Therefor special attention must be given to reduction of friction and eddy current losses in high-speed electrical machines (HSEM).

Higher harmonic content of air-gap flux density is the main source of eddy current losses in solid rotor cage induction machines. These higher harmonics are mainly caused by slotting. Generally, there are two sources of harmonics related to slotting in electrical machines. First are harmonics caused by windings concentrated in slots and another one are harmonics related to permeance variation due to slotting. The first one is dependent on the loading of machine and the second one is typically considered as load-independent. Both sources of harmonics have the same wave numbers and frequencies. This mean that these harmonics are superposing on each other. Heller and Hamata proposed in [1] following equation for the slot harmonics:

$$B_S^S(\phi^S, t) = B_+ \cos[(Q_s + p)\phi^S - \omega_s t] + B_- \cos[(Q_s - p)\phi^S + \omega_s t] \quad (2)$$

where Q_s is number of stator slots, p is number of pole-pairs, ϕ is polar angle, ω_s is synchronous angular speed, t is time and B+, B- are amplitudes of slot harmonics. First one rotates in the same direction as a main flux, second one rotates in negative direction. These harmonics have different length wave which varies at the same frequency as fundamental harmonic. Solid rotor surface is exposed to field in rotor frame of reference. After transformation from stator to rotor frame of reference the equation is as follow

$$B_r^r(\phi^r, t) = B_+ \cos\left[(Q_s + p)\phi^r + Q_s(1-s)\frac{\omega_s}{p}t - s\omega_s t\right] + B_- \cos\left[(Q_s - p)\phi^r + Q_s(1-s)\frac{\omega_s}{p}t + s\omega_s t\right] \quad (3)$$

where s is rotor slip. It can be noticed that harmonics vary at much higher frequency in rotor frame of reference than in stator frame. Therefore, slot harmonics are very efficient in producing eddy-current losses. The slot harmonics can be seen as a drop in flux density distribution in air-gap. Higher drop is resulting into the higher slot harmonics components B_+ and B_- and therefore into higher eddy current losses. Distribution of flux density above slot opening on a surface of the rotor is shown in Fig. 2a. The amplitude of flux density drop B_n can be, according to Heller and Hamata [1], derived by following equation:

$$B_n = 2\beta \; B_{max} \quad (4)$$

where B_{max} is the value of flux density without slotting and β is function of the ratio between slot opening and the radial air-gap length:

$$\beta = \frac{1 + x^2 - 2x}{2(1 + x)} \quad \text{where,} \quad x = \frac{o}{2\delta} + \sqrt{1 + \left(\frac{o}{2\delta}\right)^2} \quad (5)$$

Where o is slot opening and δ is radial air-gap length. If we assume that slot opening is o=1.5 mm then the per unit flux density drop can be expressed by function plotted in Fig. 2b. Since eddy currents are generated by changes of magnetic flux the total value of rotor eddy current losses should follow this function. Amount of eddy current losses might be significantly reduced by varying air-gap length. Therefore air-gap length has significant influence on machine efficiency with respect to equation (1).

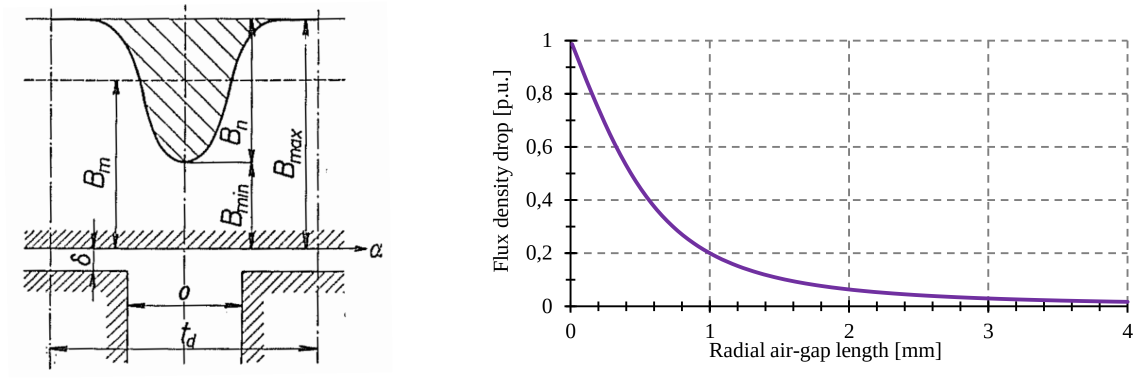

(a) (b)

Figure 2: a) Distribution of flux density above a slot [2] b) Per unit flux density drop as a function of radial air-gap length

3. RESULTS OF ELECTROMAGNETIC CALCULATIONS

Model for electromagnetic calculations has been made according to [2] in Ansys Maxwell. Performed calculations are based on time-step, 2D finite element analysis. For reduction of computation time the sinusoidal power source is considered. Impedances of end windings and short-circuit rings are modeled through external circuits. The elements dimensions close to rotor surface are smaller than the skin depth associated with slot harmonics and material characteristics. This set-up is necessary for accurate eddy current losses calculation. Skin depth can by expressed as follow:

$$\delta_{skin} = \sqrt{\frac{2}{\omega\sigma\mu}} \tag{6}$$

where ω is harmonic angular frequency, σ is electric conductivity and μ is permeability. Calculated field and rotor ohmic loss distributions are both shown in Fig 3.

Flux density drops caused by slotting can be noticed in normal component of radial flux density shown in Fig. 4a. Per unit flux density amplitudes of first- and second-order slot harmonics of the stator
(11^{th}, 13^{th} and 23^{rd}, 25^{th}) and rotor (17^{th}, 19^{th} and 35^{th}, 37^{th}) are shown in Fig. 4b. In the stator frame of reference, the stator slot harmonics vary at power supply frequency. The frequency of the rotor slot harmonics is in the kilohertz range.

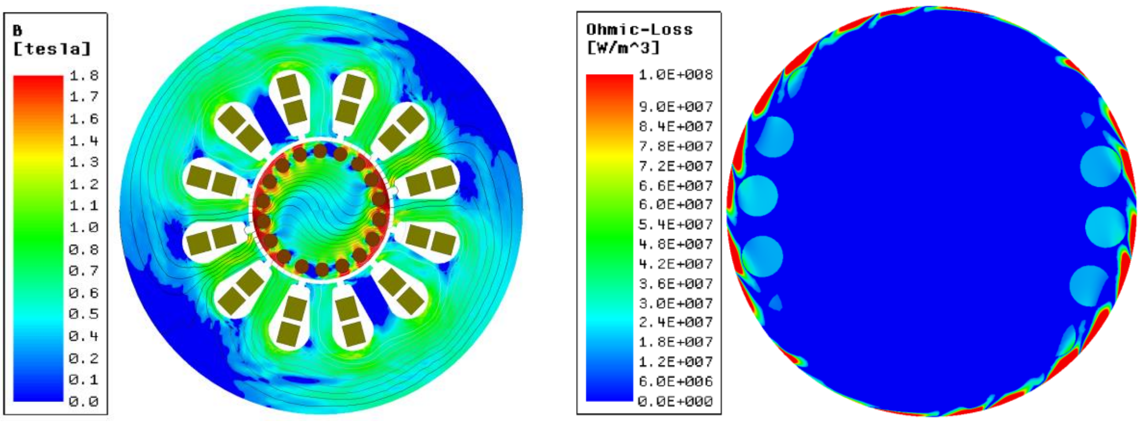

(a) (b)

Figure 3: a) Flux density distribution at the rated load condition and radial air-gap length 0.9 mm b) Ohmic-loss distribution in the rotor at the rated load condition and radial air-gap length 0.9 mm

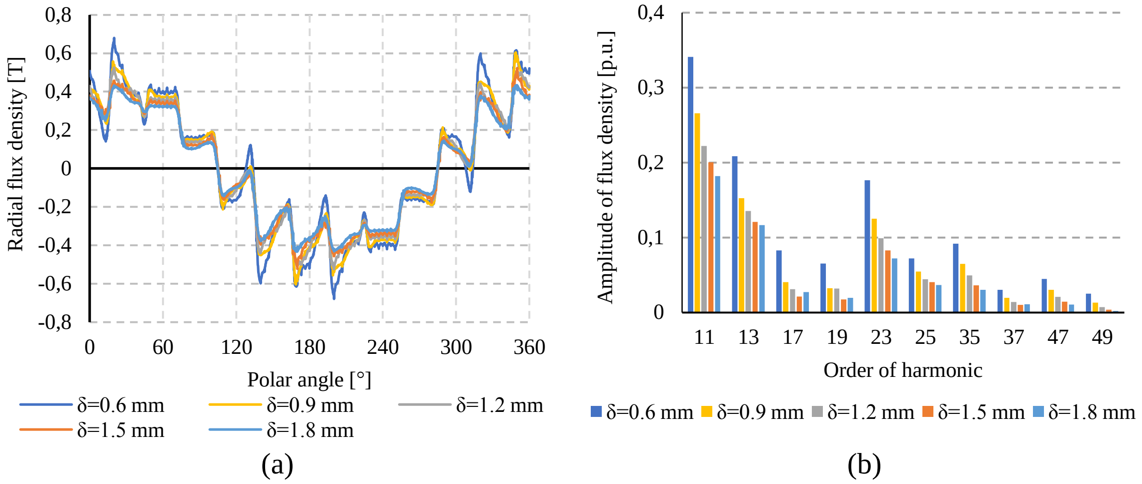

Figure 4: a) Flux density normal component distribution in the middle of the air gap b) Per unit amplitudes of the air-gap flux density slot harmonics

Calculated losses for rated load condition as a function of the radial air-gap length are shown in Fig. 5a. Results were obtain by number of iteration with thermal calculations. Iterations with thermal calculation are necessary since material resistances are thermal dependent. It can be noticed that rotor losses have similar radial air-gap length dependency as a function of flux density drop shown in Fig. 2b. It is because the eddy-current losses are decreased with smaller flux density drop. In simplified form, rotor losses dependency can be expressed as follows:

$$P_{rot} = \frac{1}{k_{rot}\delta^{x}} \tag{7}$$

where k_{rot} and x are constants dependent on motor design and δ is radial air-gap length. The stator losses increase with increase of air-gap. That is due to increase of magnetization current of the motor. Stator losses in simplified form can be expressed as follows:

$$P_{stat} = k_{stat}\delta^{x} \tag{8}$$

where k_{stat} and x are constants dependent on motor design and δ is radial air-gap length. Radial air-gap length has impact on HSSRCIM electromagnetic efficiency as is shown in Fig. 5b. However, large air-gap leads to poor power factor.

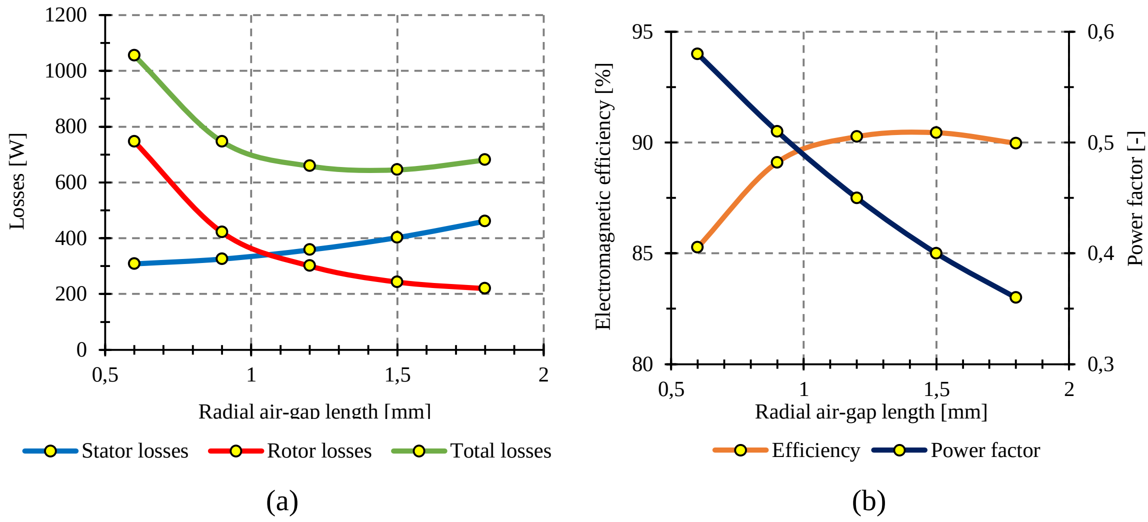

Figure 5: a) Losses as a function of radial air-gap length b) Electromagnetic efficiency and power factor as a function of radial air-gap length

4. RESULTS OF THERMAL CALCULATIONS

For internal thermal distribution, a thermal equivalent circuit has been created to model heat transfer inside the designed HSEM. The machine cooling is done through indirect water flow in cylindrical channels located inside of stator housing in combination with Helium which flows through electric machine air-gap. It is assumed that ambient temperature is 40 °C.

The calculated temperature dependency on air-gap length is shown in Fig. 6. The stator winding insulation class must be selected with respect to stator winding temperature. The rotor eddy current losses generates high temperature rise in area of rotor surface. This generated heat is efficiently removed by helium flow. Without the helium, the stator would be affected much more by rotor temperature rise.

Stator temperature is increasing for wider air-gap. That is due higher stator losses caused by poor power factor. However, it can be noticed that this temperature rise has no significant impact on temperature distribution inside electrical machine.

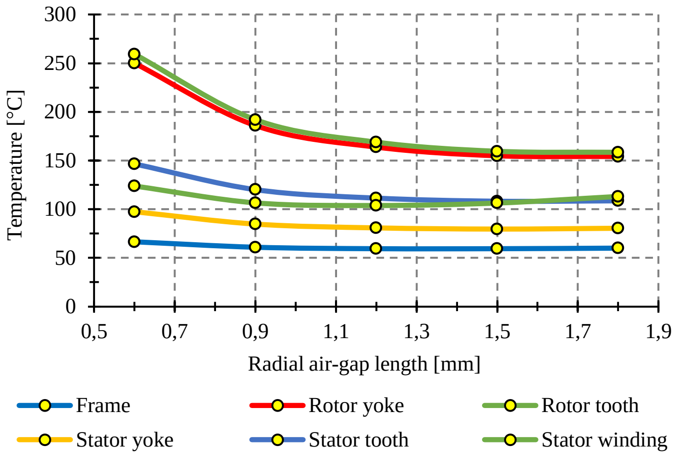

Figure 6: Temperatures as a function of radial air-gap length

5. CONCLUSION

It has been shown that significant additional losses are generated by slotting and slot harmonics in solid rotor. This paper presents reduction of their effects by using wider air-gap. Another possibility how to reduce their effects is by using closed slot, magnetic slot wedges and skewing of rotor or stator slots.

It can be concluded that air-gap design has major impact on machine performance in terms of efficiency. Presented results can therefore be used as a guideline for radial air-gap length design.

ACKNOWLEDGEMENT

This research work has been carried out in the Centre for Research and Utilization of Renewable Energy (CVVOZE). Authors gratefully acknowledge financial support from the Ministry of Education, Youth and Sports of the Czech Republic under NPU I programme (project No. LO1210)

REFERENCES

[1] Heller B., Hamata V.: Harmonics Field Effects in Induction Machines, Academia, Publishing House of the Czechoslovak Academy of Sciences, 1977

[2] Barta J., Ondrusek C., "Finite Element Analysis of High-Speed Solid Rotor Induction Machine with Copper Cage," Advanced Mechatronics Solutions, vol. 393, pp.195-200, Jan. 2016.